

UA Repository

Natural convection drying of mango slices: An experimental study

Item Type	Bachelor dissertation
Authors	Obispo, Siguerd
Citation	Obispo, S. (2026, March 23). Natural convection drying of mango slices: An experimental study. [Bachelor thesis]. University of Aruba.
Publisher	University of Aruba
Rights	Attribution-NonCommercial-NoDerivatives 4.0 International
Download date	2026-05-12 09:59:34
Item License	http://creativecommons.org/licenses/by-nc-nd/4.0/
Link to Item	https://hdl.handle.net/20.500.14473/1996

Natural convection drying of mango slices: An experimental study

Siguerd Obispo (ID:167703)
167703@student.ua.aw

Thesis supervisor: Kailas R. Malwade

**Faculty of Arts & Science, SISSTEM
University of Aruba**

Date: 23/03/2026

Abstract

Small state islands like Aruba are highly dependent on other countries for food. Vulnerable to natural calamities and impediments in food supply chain can cause difficulties and concerns to the local population. It is the need of time to focus on food security by reducing the import dependency and strengthening agriculture at local and commercial level. To strategize the focus on food security, indirect solar food dryer was tested for drying mango slices. This experimental study focused on the determination of temperature distribution within the solar dryer, drying kinetics, effect of slice thickness on drying process, and finally performance evaluation of solar dryer. The study of natural convection drying of mango slices indicated the feasibility of the drying process at existing climatic conditions. Temperature distribution within the FC indicated uniform temperature and maintained the drying air (HTF) temperature of 38 – 44 °C. It was a significant step in natural convection drying process. The drying curves were obtained to study drying kinetics and observed that maximum moisture was evaporated in the first 2 hours of drying process. The drying rate decreased in the last 4 hours of the drying process. Effect of slice thickness demonstrated decrease in drying rate as thickness increased. Thin layer modeling demonstrated Wang and Singh equation best fit with the experimental measurements. Performance evaluation of dryer showed the specific moisture extraction rate in the range of 0.07 to 0.12 kg of moisture evaporated per kWh of energy consumed.

Keywords: solar energy, drying, kinetics, moisture, evaporation

Contents

1. Introduction.....	1
2. Literature review	3
3. Research Methodology.....	5
3.1 Description of an indirect solar food dryer.....	5
3.2 Curved inlet section for natural convection drying.....	5
3.3 Thermocouple positioning.....	6
3.4 Sample preparation and positioning	7
3.5 Experimental measurements	7
3.6 Calculations	8
4. Results and Discussion.....	10
4.1 Temperature distribution	10
4.2 Drying curves.....	12
4.3 Effect of slice thickness on drying process.....	12
4.4 Thin layer modeling.....	13
4.5 Performance of SCU and the dryer.....	15
5. Conclusions	16
Future work	16
Appendix	17
References	23

List of Figures

Figure 1: Designation of solar food drying systems (Kumar et al, 2015).....	2
Figure 2: Indirect solar food dryer a) Sketch and b) Picture.....	5
Figure 3: Curved inlet air duct for natural convection drying a) Sketch, b) Picture	6
Figure 4: Thermocouple placement in the Inlet section, SCU, and FC	6
Figure 5: Positioning and array of mango slices in FC.....	7
Figure 6: Solar radiation measurements and temperature distribution in a dryer	10
Figure 8: Natural convection drying rate of mango slices for datasets 1 and 2	12
Figure 7: Moisture ratio over drying period for datasets 1 and 2.....	13
Figure 9: Comparison of experimental and predicted values for different slice thickness	14

List of Tables

Table 1: List of thin layer models employed	9
Table 2: Average temperature in the drying chamber.....	11
Table 3: R ² and RMSE for thin layer models	14
Table 4: Solar dryer performance.....	15

List of Symbols

ΔT	Temperature difference (°C)
m	Mass flow rate (kg/s)
C_p	Specific heat of material (kJ/kg °C)
W	Moisture content wet basis (kg/kg)
X	Moisture content dry basis (kg/kg)
m_w	Mass of water (kg)
m_d	Mass of solid (kg)
MR	Moisture Ratio
M_t	Moisture content at time t (%)
M_e	Moisture content at equilibrium (%)
M_0	Initial moisture content (%)
a	Constant value output from its' respective model
k	Constant value output from its' respective model
t	Time (s)
COP	Coefficient of performance (%)
Q_o	Thermal output power (W)
m_a	Airflow rate (kg/s)
T_o	Outlet temperature (°C)
T_i	Inlet temperature (°C)
A_c	Surface area of solar collector (m ²)
I	Solar radiation (W/m ²)
η_c	Collector efficiency (%)
m_e	Mass of evaporated water (kg)
h_{fg}	Latent heat of evaporation (kJ/kg)
V_{inlet}	air velocity at the dryer inlet (m/s)
V_{outlet}	air velocity at dryer outlet (m/s)
A_{inlet}	area at the inlet section (m ²)
A_{outlet}	area of the outlet section (m ²)

List of Abbreviations

PV	Photovoltaic
HTF	Heat transfer fluid
SCU	Solar collector unit
COP	Coefficient of performance
RMSE	Root means squared error

1. Introduction

Aruba, a small island state, is entirely dependent on food and energy imports. Dependence on food especially makes the population susceptible to external shocks, for example, the 2020 pandemic, and other natural calamities (UNDP, 2024). Food security is a significant concern in Aruba, driven by limited land and unfavorable soil conditions for conventional farming. Moreover, Aruba faced supply chain disruptions during the global pandemic, which negatively affected its food security. Though the local agriculture industry is moving forward at a small scale through microfinancing incentives, it still faces substantial challenges in terms of productivity due to the hot climate, infertile soil quality, and postharvest losses (Kort et al., 2024; Mohapatra & Mahanta, 2012).

Exploring economical, locally available opportunities for food drying using solar energy is one of society's greatest needs. Application of solar energy and its implementation can play a pivotal role in dealing with challenges like food security (Olabi et al., 2023). The sun is a renewable, free energy source abundantly available during the day. Aruba has 8 hours of daily sunshine and an average year-round temperature of 28 °C, making it a favorable environment for the energy-intensive food-drying process. Its effective use in food drying applications not only supports reducing the impact of climate change but also achieves the 2030 agenda for sustainable development goals (UNDP, 2025).

The high-quality, disease-free mangoes with a good shelf life result from safe production and handling practices during harvest. However, the quality cannot be improved post-harvest, and the produce needs more attention to prevent losses due to temperature and relative humidity. The mangoes produced on Aruba are a good example of a product with high postharvest losses, representing a missed opportunity for economic profit. Postharvest losses are attributed to a lack of storage capacity, inadequate handling, high perishability, and susceptibility to diseases (Schudel et al., 2023). The weather conditions, like high relative humidity and temperature in Aruba, propagate microbial growth in mangoes rapidly (Zang & Mittal, 2005), leading to spoilage, changes in texture, taste, and flavor. Additionally, solar food drying can be a potential solution to prevent postharvest losses. It is a small but positive step toward food security.

The drying process removes free and bound moisture from a product, which can be successfully achieved by selecting a relevant novel solar food dryer. The designation of solar dryers is illustrated in Figure 1. The basic classification is based on parameters such as exposure to solar radiation (direct or indirect) and air movement mode (natural or forced convection).

Open sun dryers are largely used and practiced in the agricultural industry (Vijaya Venkata Raman et al., 2012). In this category, postharvest produce is directly exposed to the sun. Though open sun drying has great potential towards water removal from a fruit slice, direct sunlight exposure can lead to discoloration and incursion of insects and microbes, which potentially can create food quality issues (Meghwar et al., 2023; Schudel et al., 2023). Thus, the category provides opportunities for advancement in drying systems (Rehman & Rubab, 2022).

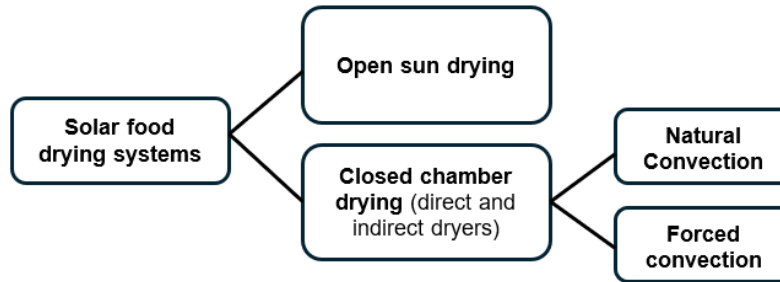


Figure 1: Designation of solar food drying systems (Kumar et al, 2015)

Closed chamber dryers overcome the limitations of open sun dryers by providing a separate food compartment (Belessiotis & Delyannis, 2011), preventing direct exposure to the atmosphere, unlike open sun drying, and preventing product quality issues. However, the closed-chamber dryers still lack uniform drying and are applicable only to small-scale drying. Both direct and indirect food dryer falls under this category of dryers (Kumar et al., 2016). With direct solar food dryers, the product is exposed to solar radiation directly but stored in a closed transparent compartment, which prevents the contaminants incursion to food items (Elwakeel et al., 2025). (Riadh et al., 2015). Indirect solar food dryers employ a solar collector unit (SCU). Convection-based heat transfer occurs from the absorber plate of SCU, heating the air as it moves over it. The heated air enters the drying chamber. This type of dryer prevents direct sunlight exposure to the food items and benefits with a high drying rate, no losses, and a lower space requirement (Belessiotis & Delyannis, 2011).

Indirect solar food dryers can be classified as: forced convection (active) and natural convection (passive) solar food dryers. Forced convection solar food dryers utilize a blower/fan to move the heated air from the SCU and pass it through the food chamber (Mugi & V. P., 2022). This external mechanism consumes electricity to move air through the dryer's different units. Passive solar food dryers operate on natural convection to move air through the dryer's different units. Wind direction and speed are consistent year-round in Aruba with sunlight intensity ($\sim 900 \text{ W/m}^2$), wind speed ($\sim 21 \text{ mph}$), and wind direction (91.5% East, 8.5% East-southeast) (DM Aruba, 2020). Aruban agriculture is currently in development, and as a result, mango cultivation and production are not yet commercialized. However, mango trees are commonly grown in households because of their suitability for warm, sunny climates. Most of the mangoes, during mango season, end up on the ground or are eaten by birds. On the other hand, large volumes of mangoes harvested over a short period can lead to spoilage. Thus, it presents a great opportunity to address the existing gap in mango harvest and postharvest losses by testing a natural convection food dryer to prevent spoilage.

The thesis primarily focuses on the following objectives: 1) investigating the thermal performance of the solar food dryer without loading mango samples in the food chamber, 2) the effect of slice thickness on the drying rate of the mangoes, and 3) evaluation of indirect solar food dryer performance.

2. Literature review

The literature review provided a brief overview of previous studies, findings, and developments in food dryers. Previous studies provide a useful tool for understanding current research trends and for gaining insight into various external parameters that affect drying performance: airflow rate, air temperature, humidity, slice thickness, slice diameter, and air inlet design, which need to be considered when designing an experimental plan. The drying process varies uniquely depending on the food product, and so does the mechanism. Hence, thin-layer modeling is crucial for making accurate calculations and predictions. These models were therefore studied using experimental measurements.

(Ennissioui et al., 2023) reported experimental study of natural convection drying of banana slices at Moroccan geographical and climatic conditions using an indirect solar food dryer. During the drying process, the SCU recorded a maximum temperature of 58 °C, while the layered trays in the drying chamber reported an average temperature of 44 °C. The drying process reduced moisture content to 93-99%, depending on the tray location. The authors reported improved dryer performance based on previous similar studies and offered valuable insights into natural convection drying as a sustainable solution for preserving food.

An experimental study on a natural convection solar greenhouse dryer for domestic usage was reported by (Tawfik et al., 2023). In this experimental investigation, the authors focused on a controlled natural convection drying mode using a solar greenhouse dryer to dry grapes via intermittent operation with a PV system. Two types of materials, glass and Plexiglas, were used to build the dryer. The authors claimed that natural convection drying results with plexiglass as a cover material are equivalent to those of forced convection drying. Almost the entire moisture (97 %) was removed from grapes in 12 hours using a controlled natural convection drying mode in a solar greenhouse dryer. It reported the same moisture reduction percentage by natural convection drying mode but took 15 hours to dry. This difference in drying time was caused by a DC fan installed to serve as an exhaust. The authors stated that the new controlled natural convection drying mode is a good alternative to the forced convective drying method.

(Mimmi et al., 2025) evaluated a newly developed natural convection solar dryer for drying cabbage. Cabbage samples were prepared by blanching with NaCl and dried in the open sun and in a solar dryer at 55.67 °C for 12–16 sunshine hours. However, the authors compared the drying rates of single-layer and multilayer cabbage samples, with single layers showing a higher rate. On the other hand, the drying efficiency of multilayer cabbage samples was reported to be higher than single-layer cabbage samples. The best-fit model was the Page model for single- and multilayer cabbage sample experiments.

(Getie et al., 2025) investigated a direct solar dryer to dry onions by evaluating efficiency, drying rate, and uniformity of temperature (Getie et al., 2025). The results of the direct solar dryer were compared with those of open sun drying. During the drying process, the temperature in the food chamber was 3–5 °C above ambient. Getie et al. reported a total drying time of 77 h for onions, with a drying rate of 0.024 kg/h in the direct solar dryer, twice that of open-sun drying. Thin-layer modeling was conducted, and the Page model best fits the experimental data in describing onion behavior during drying.

Most common designs of natural convection inlets consist of a uniform rectangular cross-sectional duct throughout its length, with a glass cover on the top (Singh et al., 2019). Singh et al. further

argue that while other studies use methods to increase the ΔT in the energy gain formula ($m \times C_p \times \Delta T$), this approach comes at the cost of reduced mass flow rate m , which limits the effectiveness of solar collector systems to a short period. Singh proposes using a bell-mouth air inlet to improve air flow and thus a higher flow rate (m). Singh et al found that a bell-mouth design increases mass flow by a maximum of 18% compared to a traditional rectangular cross-section at a solar flux of 500-1100 W/m². The bell-mouth design also showed greater solar energy conversion, resulting in greater savings in sunlight hours. These studies suggest that the bell-mouth air inlet is a suitable design to integrate into the natural convection solar dryers. Bell-mouth air inlet designs have been proven to increase air flow efficiency in natural convection drying applications (Park et al., 2025).

From the literature review above, it was observed that direct, indirect, and open-sun drying are commonly used to dry fruits and vegetables. However, further design modifications are necessary to test the food dryer under Aruban weather conditions. In this thesis, an air inlet section was designed with two openings on either side of the food dryer, as shown in Figure 3 to speed up the natural convection drying of mango.

3. Research Methodology

3.1 Description of an indirect solar food dryer

The indirect solar food dryer, as shown in Figure 2 consisted of an inlet section, solar collector unit (SCU), food chamber made of transparent plexiglass (FC), outlet section, and data acquisition system. Natural air as heat transfer fluid (HTF) entered from the inlet section and moved through the SCU. Incoming solar radiation hit on a black-painted absorber plate (1.2 m x 0.5 m x 0.002 m) surface installed inside the SCU. The plate surface absorbed radiation and converted them into heat. HTF was moved over and beneath the plate and heated through a natural convection heat transfer mechanism and moved further into an FC perpendicular (cross flow) to the array of mango slices, supported by the perforated metal tray. HTF finally exited through the outlet section. Honeycomb sheets were installed at the inlet and outlet of the SCU, and just above the food chamber, to maintain uniformity in the HTF flow. SCU and its connections were insulated to prevent heat loss. The picture and sketch of the indirect solar food dryer are shown in Figure 2.

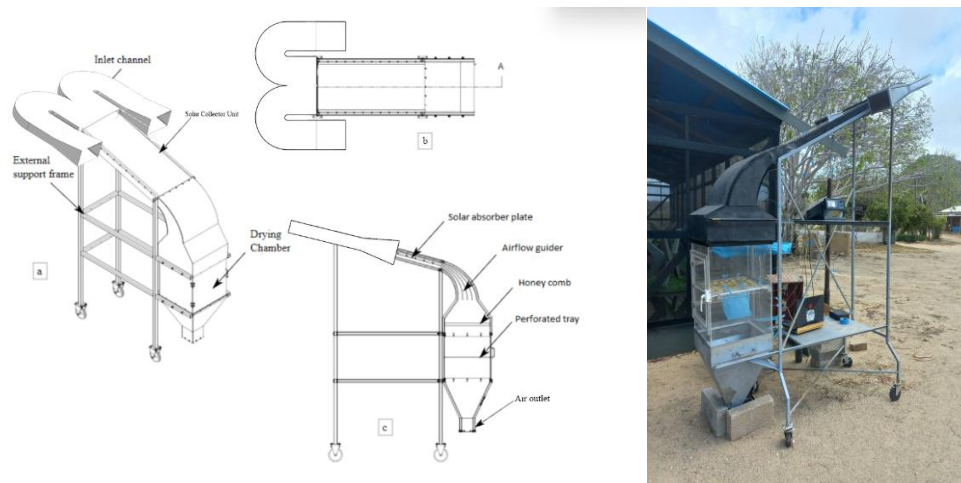


Figure 2: Indirect solar food dryer a) Sketch and b) Picture

3.2 Curved inlet section for natural convection drying

The paramount wind direction in Aruba blows regularly at an average speed of ~21 mph from the east to north-east direction throughout the year. Such year-round climatic conditions benefits and favor natural convection drying. The inlet air duct was designed in such a way that the predominant wind direction and maximum incoming solar radiation occur during the drying process. A curved inlet section was connected to the SCU, facing in the opposite direction to the wind, to capture and move the HTF through the dryer, achieving a natural convection drying. The 2 split openings (0.25m x 0.07m each) merge near the connecting point, facilitating the capture of incoming air through either side entrance and lower the possible turbulence. The screens were placed on both openings to prevent intrusion of dust, insects, and other contaminants. A visual representation of the curved inlet section is shown in Figure 3.

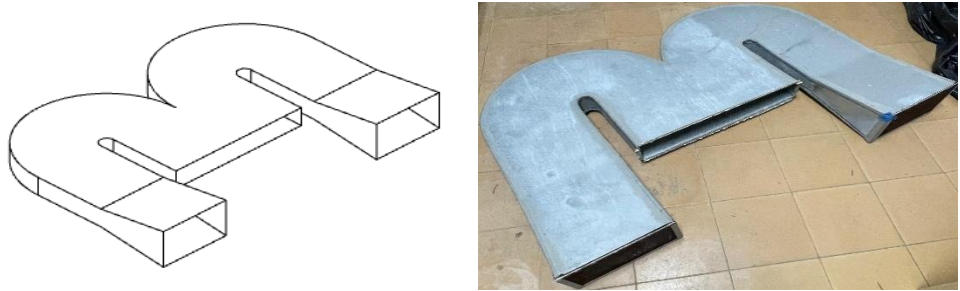


Figure 3: Curved inlet air duct for natural convection drying a) Sketch, b) Picture

3.3 Thermocouple positioning

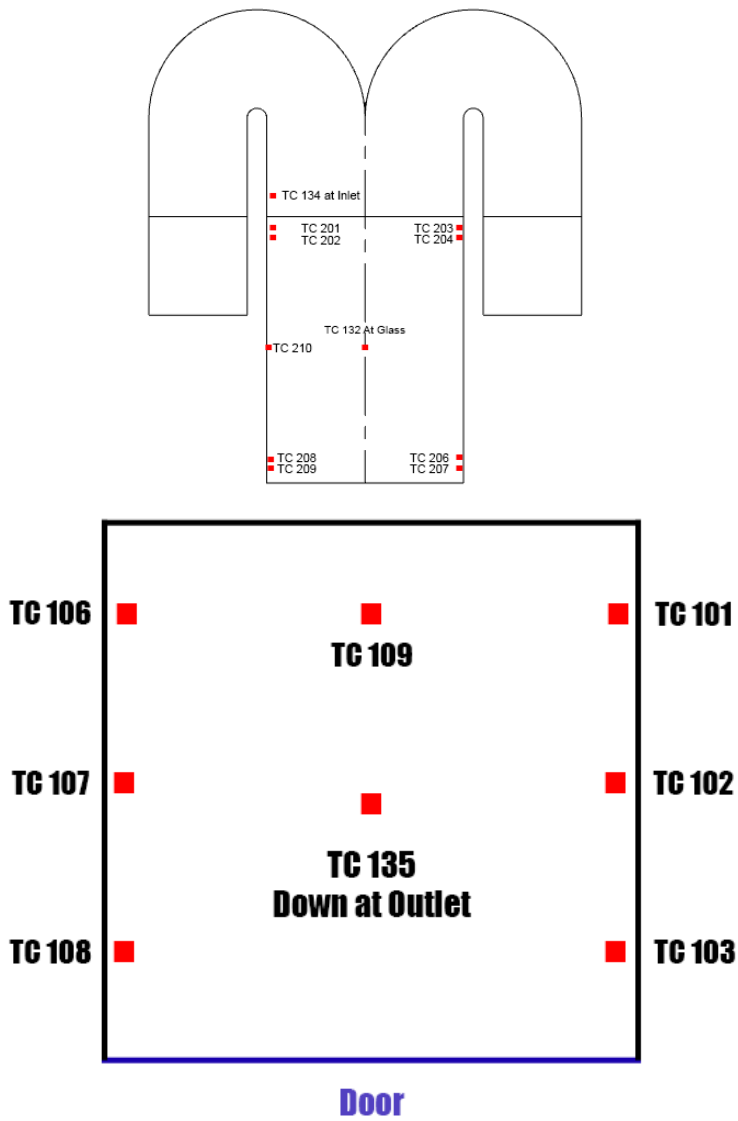


Figure 4: Thermocouple placement in the Inlet section, SCU, and FC

Figure 4 provides insight into the placement of 20 thermocouples across the indirect solar food dryer: 9 in the SCU, 7 in the FC, and 4 in the inlet/outlet section. The thermocouples were calibrated using a temperature-controlled bath to determine the voltage direct current (VDC) corresponding to each temperature. The calibration curve included in the appendix. The thermocouples were wired to a multiplexer and connected to a data logger, which recorded the VDC corresponding to each thermocouple's temperature every 10 seconds. The data logger was connected and controlled by the device software installed on the on-site laptop for real time measurements.

3.4 Sample preparation and positioning

The mangoes were purchased from Ling and Sons, a local supermarket, and washed, then cut into uniform slices using a professional slicer. Slices 3, 4, and 5mm thick and 20 mm in diameter were used for the drying experiments. Each slice was weighed and placed into the FC as shown in Figure 5. A total of 40 discs were placed in the drying chamber in an 8 x 5 grid, with each slice occupying a specific spot throughout the experiment.

01 02 03 04 05
 06 07 08 09 10
 11 12 13 14 15
 16 17 18 19 20
 21 22 23 24 25
 26 27 28 29 30
 31 32 33 34 35
 36 37 38 39 40

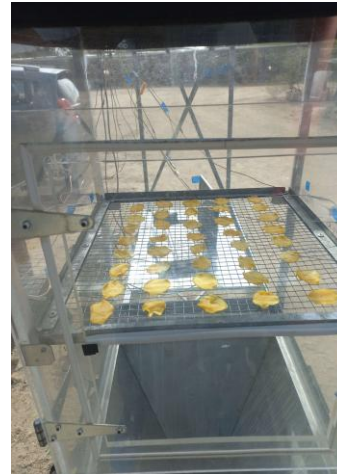


Figure 5: Positioning and array of mango slices in FC

3.5 Experimental measurements

Incoming solar radiation was measured during each experiment using a pyranometer at every 15 minutes. The airflow at the dryer outlet was measured and recorded to calculate the inlet velocity using equation 1 below:

$$V_{inlet} = \frac{V_{outlet} \times A_{outlet}}{A_{inlet}} \quad (1)$$

Measurements were initially carried out for 6 hours from 10:00 am to 4:00 pm, unloading mango slices, by recording temperature in SCU, FC, inlet, and outlet sections of the dryer. All the real-time measurements were conducted during daytime for 3 consecutive days and stored through the data acquisition system.

The drying experiments were performed by placing an array of mango slices (40 numbers). The effect of thickness was investigated at 3, 4, and 5 mm thick mango slices. The drying experiments were carried out, following a similar schedule as that of first part of temperature measurements. Every 2 hours, the mango slices were weighed and recorded to calculate the drying rate and get the moisture content later in data analysis. After 6 hours of drying, the samples were weighed again and placed in an electric oven overnight at 45 °C to obtain the bone-dry weight of each slice. Solar intensity varied with cloud cover, and if rain was expected, the experiments were aborted to protect the equipment from water damage.

3.6 Calculations

3.6.1. Moisture content

Moisture content of a food sample consisted of both bound and unbound moisture available (Belessiotis & Delyannis, 2011). It is commonly expressed on a wet basis (W) or dry basis (X). Moisture content on wet basis means the moisture mass with respect to the mass of the wet material, whereas dry basis means the moisture mass per bone dry mass of material (Meghwar et al., 2023).

$$W = \frac{m_w}{m_w + m_d} \quad (2)$$

$$X = \frac{m_w}{m_d} \quad (3)$$

As the moisture content is a temperature-dependent quantity, it changes over time during the drying process. It's important to estimate the quantity of water left in the product relative to the amount it had at the beginning during the drying process, which was achieved by measuring the weight of each slice at 2-hour intervals. Thus, moisture ratio (MR) was considered and calculated as follows (Ren et al., 2025):

$$MR = \frac{M_t - M_e}{M_0 - M_e} \quad (4)$$

3.6.2 Thin-layer modelling

Drying kinetics can be modeled with mathematical models. Thin-layer modelling is commonly used to predict and describe the drying process of produce. Models can be used to optimize the solar dryers and the drying parameters (Tepe, 2024). In thin-layer modeling, the drying rate is dependent on drying temperature, moisture content, and the properties of the product, such as size and thickness (Belessiotis & Delyannis, 2011). There are several thin-layer models to describe the drying behavior of all products. Experimental values were validated using mathematical models to determine the optimum model. An R-squared value close to one is used to determine the best-fit model. A list of mathematical models used in this investigation is stated in Table 1.

Table 1: List of thin layer models employed

Model	Formula	References	
Henderson & Pabis	$MR = a \times \exp(-kt)$	(Henderson & Pabis, 1961)	(5)
Newton	$MR = \exp(-kt)$	(El-Beltagy et al., 2007)	(6)
Wang & Singh	$MR = 1 + at + bt^2$	(Omolola et al., 2014)	(7)

3.6.3 Statistical indices for model selection

Evaluation of statistical indices such as the coefficient of determination (R^2) and root mean square error (RMSE) was performed. R^2 values defined the portion of the total variation explained by regression (Caballero-Cerón et al., 2015) and closer the R^2 values to 1 described the best-fit model. RMSE was attributed to the measurement of deviation between experimental and predicted values and was estimated using equation 8.

$$RMSE = \sqrt{\sum_{i=1}^n (X_{i,predicted} - X_{i,exp})^2} \quad (8)$$

3.6.4 Performance evaluation of solar dryer

Solar energy utilized to heat a black painted absorber plate placed in SCU of solar dryer. Absorber plate surface converts absorbed solar energy to heat energy through natural convection. The HTF is then moved over the food layer to remove the moisture from mango slices. How much heat energy was utilized through natural convection drying of mango slices defines the performance of coefficient. COP of the drying system, as stated in equation 11, is the energy consumed by the product compared to the total energy supplied to the product. This shows the total energy required to remove moisture from the product.

The relationship stated in equations 9 and 10 represents the thermal output power and solar collector efficiency (Shalaby & Bek, 2014).

$$\text{Thermal output power} \quad Q_o = m_a C_p (T_o - T_i) \quad (9)$$

$$\text{Solar collector efficiency} \quad \eta_c = \frac{Q_o}{A_c \times I} \quad (10)$$

$$\text{Coefficient of performance} \quad COP = \frac{m_e \times h_{fg}}{I \times A_c \times t} \quad (11)$$

4. Results and Discussion

This section discusses the experimental outcomes of natural convection drying of mango slices, focusing on the temperature profile within the solar dryer, drying curves, and the performance evaluation of the solar food dryer.

4.1 Temperature distribution

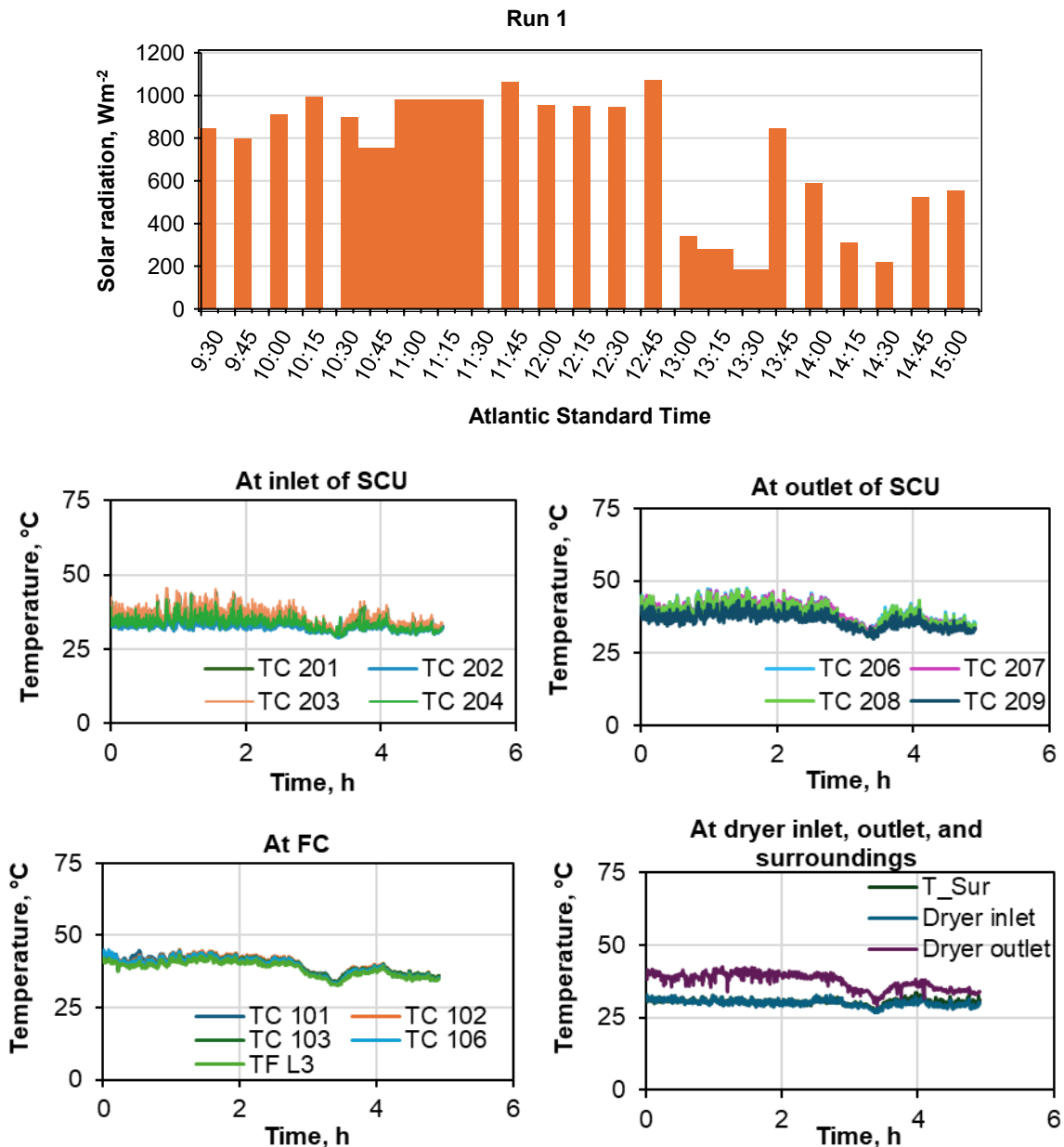


Figure 6: Solar radiation measurements and temperature distribution in a dryer

Figure 6 depicted the pattern of solar radiation measurements and temperature profile at inlet and outlet of the SCU, FC, and dryer inlet and outlet. It was observed that incoming solar radiation

onsite was consistent till 12:45 pm, then fluctuation occurred between the lowest values of 187 W/m² and 589 W/m² because of cloud cover on that day. The reduction in solar radiation intensity was, as a result, reflected in temperature profiles of different units of the solar dryer. The average temperature at the inlet and outlet of SCU was observed at 34 °C and 38 °C respectively. At the same time, the average temperature in the FC and dryer outlet was measured 38 °C. The dryer inlet and ambient temperature were reported to be relatively same of 30 °C. The temperature profile in the FC was very consistent when the SCU was fully exposed to the sun. However, a cloud cover impede the sun exposure to the SCU, causing a slight dip in temperature after 1 AST.

The temperature inside the FC was measured and recorded during daytime consecutively for three days and represented in Table 2. These experiments were carried out to determine the temperature distribution pattern maintained in the drying chamber. The temperatures in the drying chamber were measured at the center, left, and right sides.

Table 2: Average temperature in the drying chamber

		Run 1	Run 2	Run 3
TC	TC position	Average temperature (°C)		
TC 101		40.13	41.98	44.09
TC 102	Right side	40.11	42.18	44.34
TC 103		39.86	41.66	48.53
TC 109	Center	40.97	43.29	47.17
TC 106		39.33	41.23	43.45
TC 107	Left side	42.02	40.99	43.52
TC 108		38.68	40.53	42.87

Thermocouple positions in the drying chamber were already mentioned in Figure 4. It was observed from Table 2 that the temperature distribution was consistent. In run 3, the temperature distribution was more uneven compared to experiments 1 and 2, with a maximum temperature difference of almost 5 °C. This trend occurred because the left side of the setup receives slightly less sunlight than the right side, as the sun is slightly to the right side of the setup for most of the experiment. Another reason for the temperature disparity could be consistent change in wind speed entering into the drying chamber. Overall, the temperature difference in all three experiments was attributed to measurement of temperature data in three different days with variation in wind speed entering the dryer and solar radiation hitting the SCU.

Solar radiation measurements and temperature distribution in a dryer for run 2 and run 3 were mentioned in Appendix.

4.2 Drying curves

The drying curves were plotted for three different slice thickness for datasets 1 & 2 as shown in Figure 7. It was noticed wet mango slice was initially heated to an exposed surface temperature equivalent to wet-bulb gas temperature, causing the evaporation of moisture at an increasing rate. The exposed slice surface was barely covered by a film of moisture after 2 hours, which indicated the drying rate reached at a point called critical moisture content of mango sample.

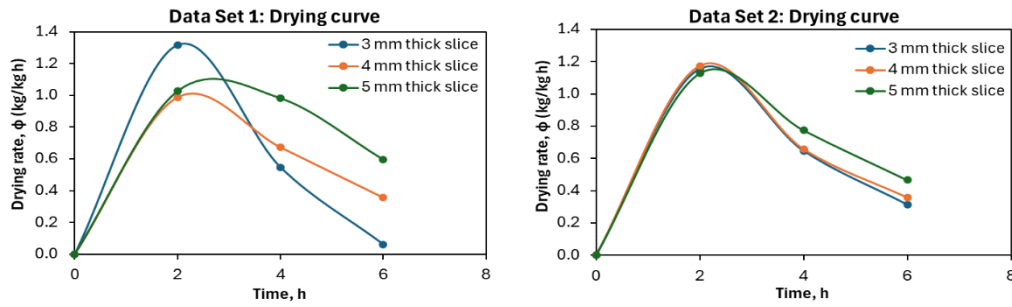


Figure 7: Natural convection drying rate of mango slices for datasets 1 and 2

The average critical moisture content of the sample was recorded as 2.26, 2.61, and 2.92 kg of moisture per kg of dry solids for 3 mm, 4 mm, and 5 mm thick slices respectively. As the drying process continued further for 4 hours, the moisture content continuously lowered and reached at the lowest average value of 0.29, 0.76, 1.27 kg/kg for 3 mm, 4 mm, and 5 mm respectively. This continuous lowering of the moisture from 2 to 6 hours during drying process is called falling rate drying period. The drying rate was initially spiked up till 2 hours and reached at a point of critical moisture content with 58, 43, and 33 % moisture removal for 3, 4, and 5 mm slice thickness respectively. However, the moisture removal of 35, 40, and 41 % occurred for 3, 4, and 5 mm slice thickness respectively. The lower moisture removal percent with longer drying time observed because the moisture within the mango matrix traveled to the surface first then evaporated. After critical moisture content point, the removal percent found in ascending order due to an effect of slice thickness.

4.3 Effect of slice thickness on drying process

To evaluate effect of slice thickness on drying process, the mango slices of 3 mm, 4 mm, and 5 mm thickness were dried by natural convection. Effect of slice thickness is shown in Figure 8 and learned from datasets 1 and 2 that the moisture ratio plummeted for 3mm thick slice and reached closer to zero. However, increase in slice thickness indicated slower moisture removal from the slices, as a result longer time required to dry by leaving higher amount of moisture within mango matrix of the respective slice.

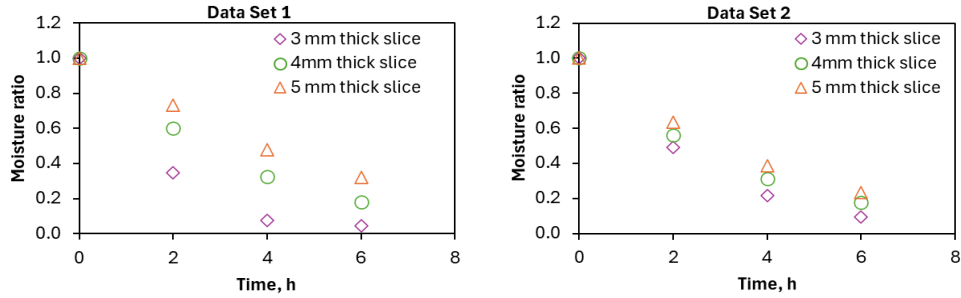
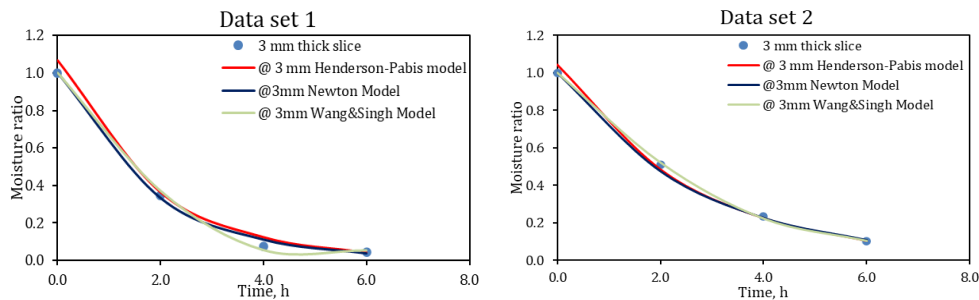


Figure 8: Moisture ratio over drying period for datasets 1 and 2

The heat transfer from HTF to 3 mm slice indicated faster compared to 4 and 5 mm thick slices. Moisture ratio of 0.04, 0.17, and 0.32 were observed after 6 hours of drying. Both datasets were measured and recorded on different days, causing a significant difference in moisture ratio occurred for each slice thickness of dataset 1, whereas the moisture ratio decreased consistently from higher to lower thickness of the mango sample. This nature of drying could be attributed to cloud cover and variation in solar intensity and natural wind speed during drying process. Similar drying phenomena was experienced by the previous investigators.

4.4 Thin layer modeling

Thin layer drying models are important mathematical tools, which can be applied to study the drying kinetics of agricultural products such as fruits, grains and vegetables (Werner Mühlbauer & Joachim Müller, 2020). It is highly important to analyze and describe thin layer modeling for optimizing the drying process, enhancing energy efficiency and maintaining the food quality (Buzrul, 2022). In this research the available semi-theoretical and empirical models were proposed to determine the best fit model with the experimental measurements. Two semi-empirical Newton/Lewis and Henderson Pabis models and one empirical Wang and Singh model were applied to fit the measurement data. The slope and intercept were initially determined initially from the linear plots moisture ratio vs time. The constants a and k from the Newton and Henderson and Pabis models were estimated using the linear regression analysis. The constants a and b for the wang and Singh model was estimated through a 2nd order polynomial regression. The drying experimental data was compared with the modeling data to validate the best fit model using coefficient of determination (R^2) and RMSE was represented in Table 3.



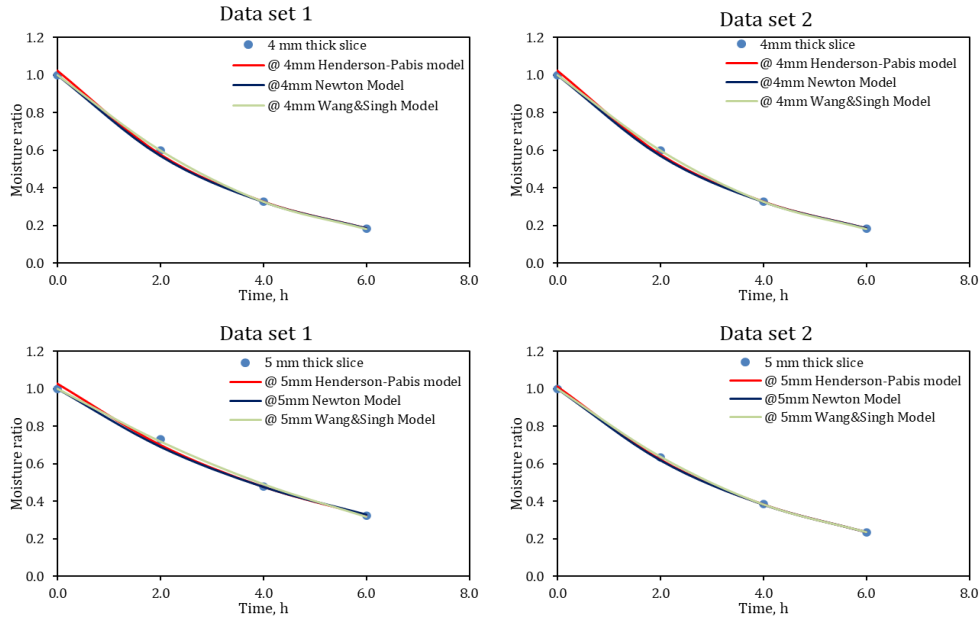


Figure 9: Comparison of experimental and predicted values for different slice thickness

The value of R^2 closer to unity and lower RMSE describes the best-fit model. The RMSE measures the difference between values predicted by the model and observed values; means the model values are closer to observed values. Figure 9 depicted the moisture ratio vs time by comparing the drying experimental data with modeled data for 3 mm, 4 mm, and 5 mm thick mango slices. Furthermore, figure 9 indicated the R^2 and RMSE values for all three models.

Table 3: R^2 and RMSE for thin layer models

Model	Henderson & Pabis		Newton		Wang & Singh		
	Run	R^2	RMSE	R^2	RMSE	R^2	RMSE
3 mm		0.998	0.037	0.998	0.006	0.998	0.005
		0.998	0.008	0.998	0.018	0.999	0.003
4 mm		0.998	0.003	0.998	0.014	0.999	0.000
		0.971	0.001	0.974	0.035	0.998	0.004
5 mm		0.994	0.002	0.994	0.019	0.998	0.003
		0.999	0.001	0.999	0.005	0.999	0.001

At the beginning of the experiment, the Henderson-Pabis model has an issue throughout all runs, as it consistently shows a moisture ratio above 1, which is physically impossible. This means that the model might not be well-suited for the initial drying period. It was observed from table 3 that the R^2 values for all models were 0.99, which made difficult to choose the best fit model. Therefore, the RMSE values were estimated indicating the better fitment of a model with higher accuracy and Wang and Singh model represented the lowest RMSE values compared with other two models. Therefore, the Wang and Singh model was the best fit with drying experimental data, showing the most optimum results to model drying kinetics of mangoes.

4.5 Performance of SCU and the dryer

Performance of the SCU was estimated by applying equations 9 and 10 for three no-load experiments performed on three consecutive days. It demonstrated the highest efficiency of SCU of 49.29 % and decreased with decrease in airflow rate. An increase in airflow rate increased the heat transfer coefficient, triggering higher efficiency of SCU. Run 1 as shown in Table 4, has a higher average airflow rate but a lower average solar intensity, being 740 W/m² or 7.6 % lower than experiment 3, but it benefits from a 57.5 % higher average airflow rate compared to experiment 3. The COP was absent from the no-load experiments, as there are no loading of an array of mango slices in the FC.

Table 4: Solar dryer performance

	No load experiments			Load experiments					
	Run 1	Run 2	Run 3	3 mm		4 mm		5 mm	
				Run 1	Run 2	Run 1	Run 2	Run 1	Run 2
Average inlet temperature, °C	30	31	31	29	30	29	29	29	29
Average outlet temperature, °C	38	39	39	36	36	35	35	35	36
Average thermal output of SCU (J/s or W)	219	220	140	136	138	84	90	92	122
Average flow rate, kg/s	0.0282	0.0276	0.0179	0.0198	0.0228	0.0135	0.0156	0.0152	0.0186
Average solar radiation, I (W)	444	520	478	386	381	265	361	436	377
Total mass of evaporated water (kg)				0.16	0.19	0.20	0.21	0.31	0.25
Average efficiency of SCU (%)	49.29	42.37	29.34	35.13	36.28	31.72	24.93	21.20	32.33
Coefficient of performance, COP (%)				4.37	5.18	7.80	6.18	7.38	6.88

The efficiency of SCU varied from 21.2% up to 36.28 % for drying experiments. The experiment with the lowest efficiency of SCU had the highest average solar radiation, but the lowest recorded airflow rate of all 9 experiments. The drying time for all experiments was equal, it was however important that drying rate for slices slowed down significantly between 4 and 6 hours, suggesting some samples reached the equilibrium state. The longer time spent on drying the mango slices indicates the lower COP. This means the more energy is utilized to remove the moisture from the mango slices, upon longer measurement time. However, the estimated COP for the natural convection drying experiments ranged from the lowest 4.37 % to highest 7.80 % because the airflow rate and solar radiation intensity kept varied during each experiment.

Thus, the specific moisture extraction rate for natural convection drying measures the effectiveness of the dryer in terms of energy efficiency, which was observed in the range of 0.07 to 0.12 kg of moisture evaporated per kWh of energy consumed.

5. Conclusions

The study of natural convection drying of mango slices indicated the feasibility of the drying process at solar radiation intensity of average of 800 W/m^2 and wind speed of ~ 19 mph during daytime. Temperature distribution within the FC maintained the drying air (HTF) temperature of $38 - 44 \text{ }^\circ\text{C}$. It was a significant step in natural convection drying process.

The drying curves indicated maximum moisture was evaporated in the first 2 hours of drying process. The drying rate decreased in the next 4 hours because the moisture within the mango matrix diffused to the surface of the slice to evaporate. The drying rate of mango slices decreased as thickness increased, which indicated the longer time required to diffuse the moisture within mango matrix to the surface. Thin layer modeling demonstrated Wang and Singh equation best fit with the experimental measurements.

Efficiency of the SCU unit varied between $21 - 36 \%$ for the drying experiments, however it was reported higher efficiency of the SCU unit for no loading experiment. This indicated very low pressure drop caused to move the HTF quickly. COP for solar dryer estimated in the range of $4 - 8 \%$, which demonstrated that the specific moisture extraction rate in the range of 0.07 to 0.12 kg of moisture evaporated per kWh of energy consumed.

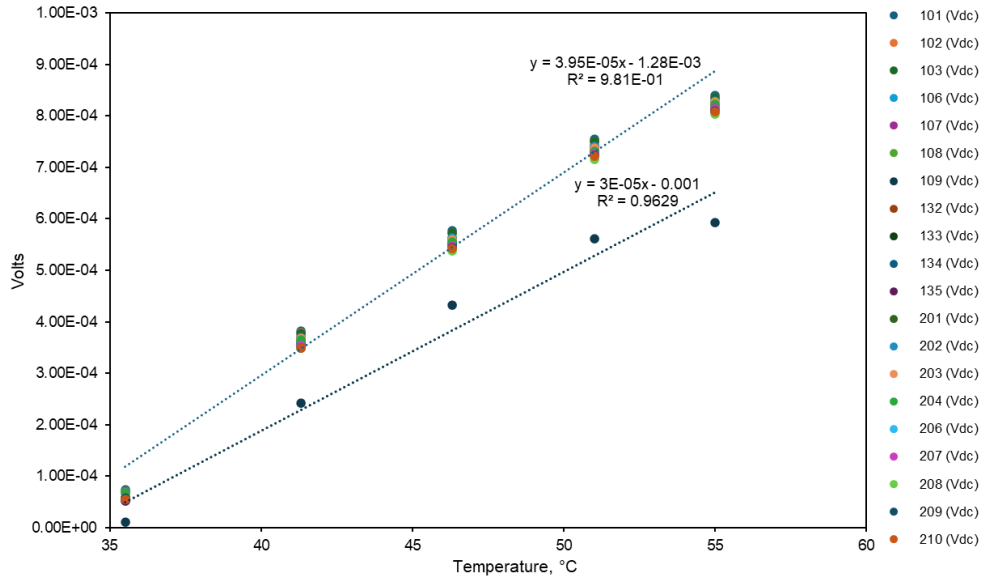
Natural convection drying of mango slices collectively not only provides a sustainable solution to the energy intensive heating process but also offers agro economic opportunities along with food security.

Future work

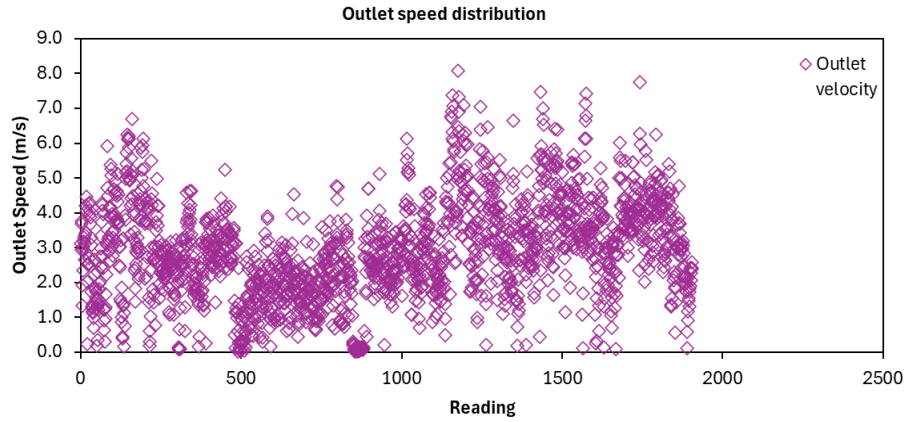
1. An improvement in the efficiency of SCU further can be achieved by providing double glass to SCU.
2. Multiple racks can be placed inside the FC to increase the drying capacity of the existing apparatus.
3. Testing of the existing apparatus in all seasons to determine the temperature distribution within the FC.

Appendix

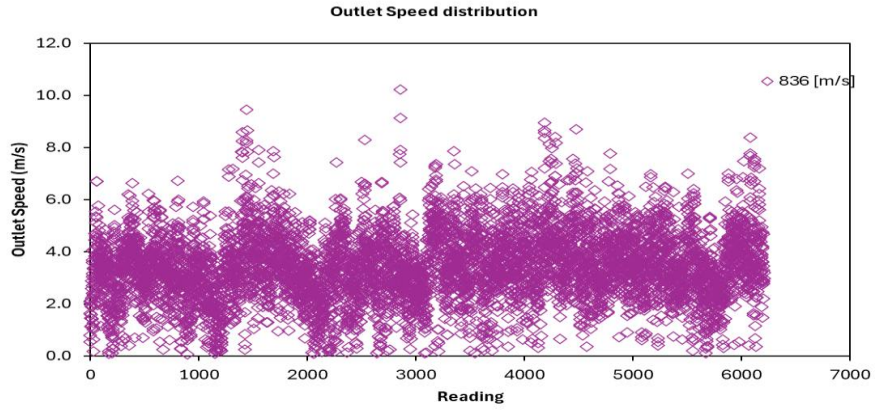
Appendix A: Thermocouple calibration curve



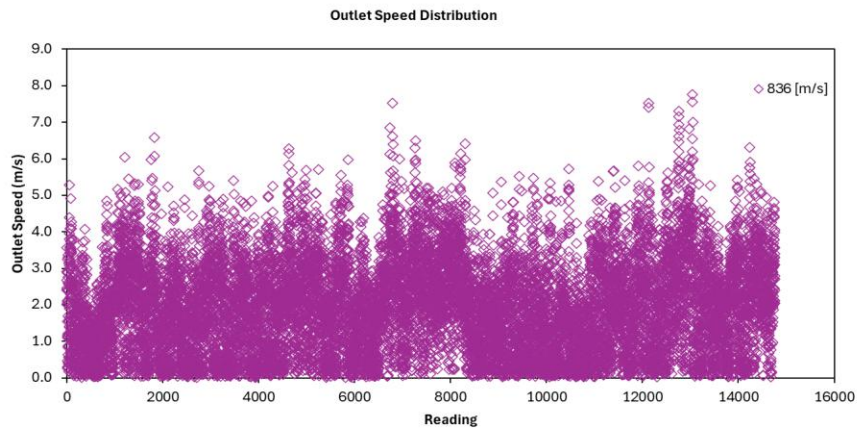
Appendix B: Outlet speed distribution



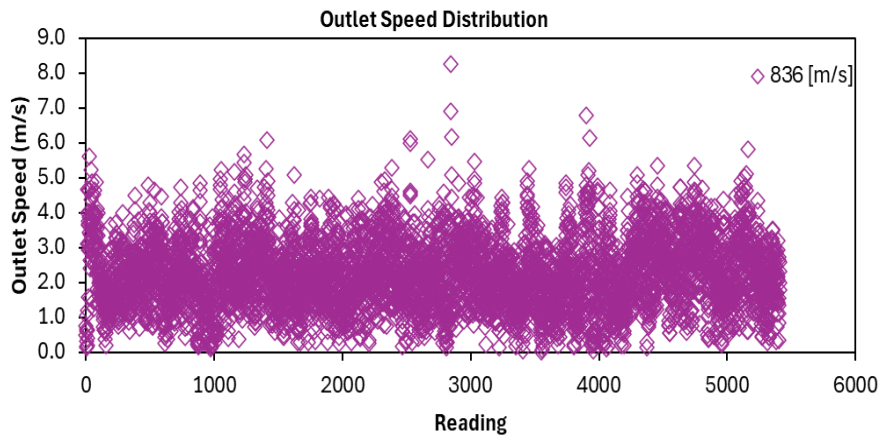
Outlet speed distribution of no-load experiment (Run 1)



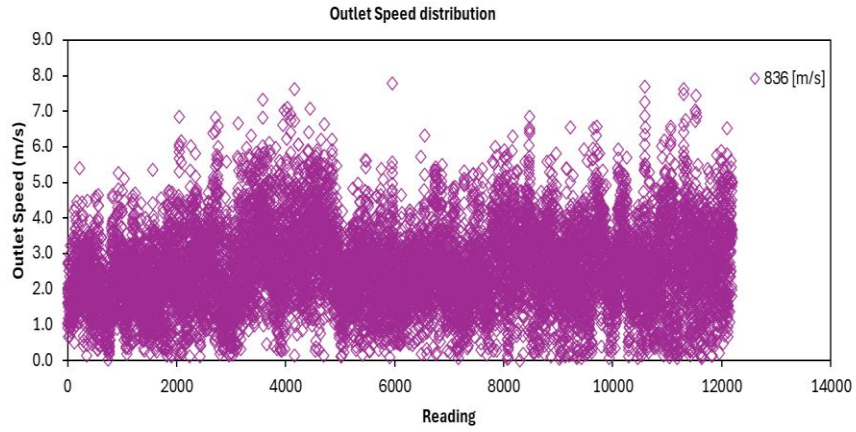
Outlet speed distribution of no-load experiment (Run 2)



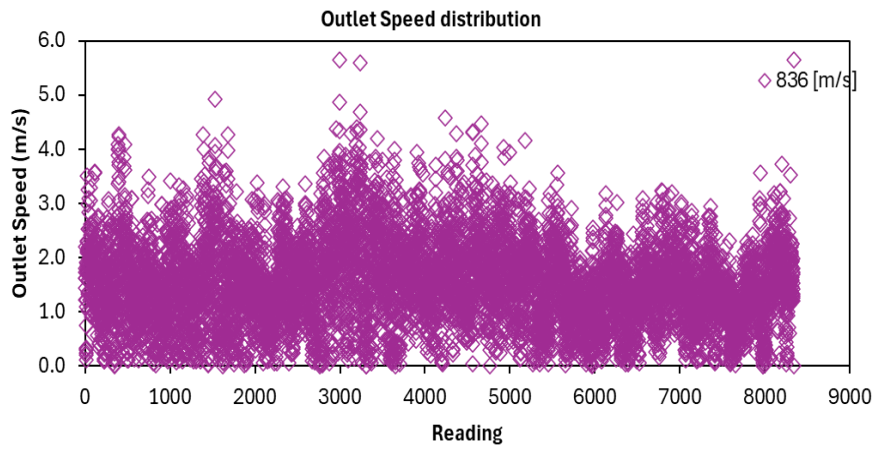
Outlet speed distribution of no-load experiment (Run 3)



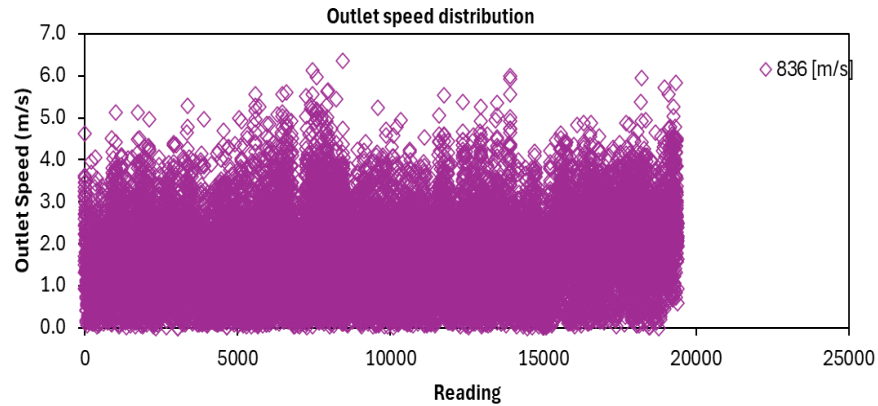
Outlet speed distribution while drying 3 mm thick sample (Run 1)



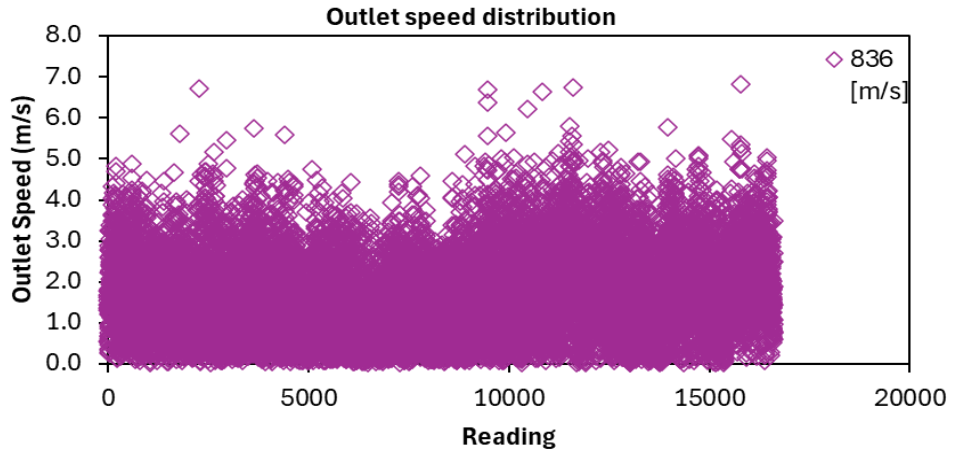
Outlet speed distribution while drying 3 mm thick sample (Run 2)



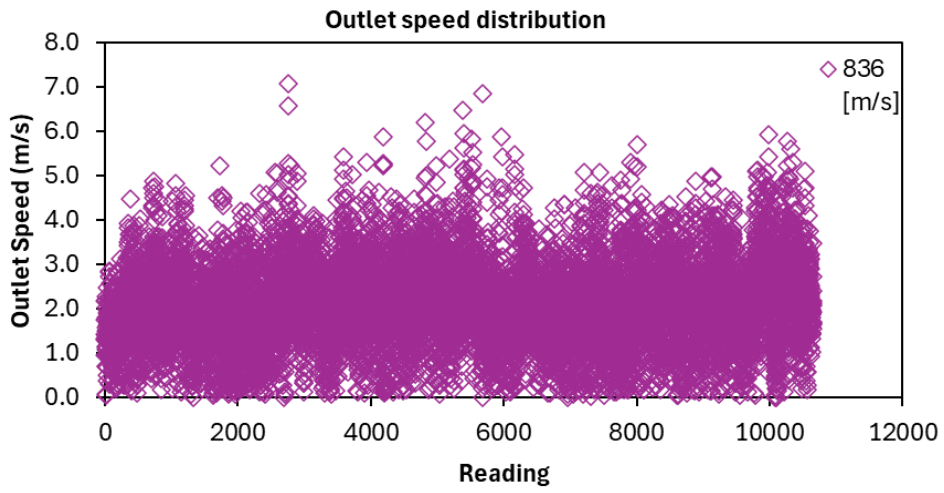
Outlet speed distribution while drying 4 mm thick sample (Run 1)



Outlet speed distribution while drying 4 mm thick sample (Run 2)

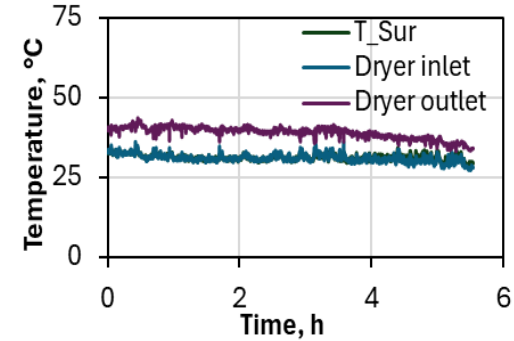
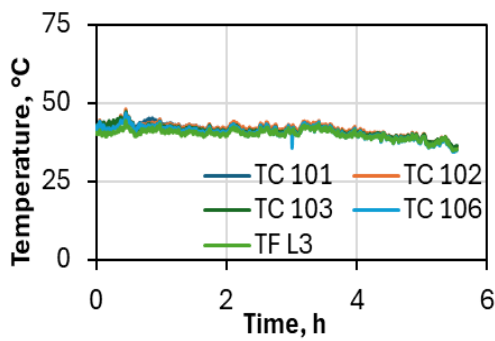
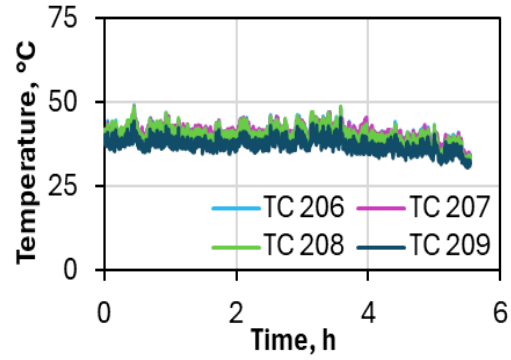
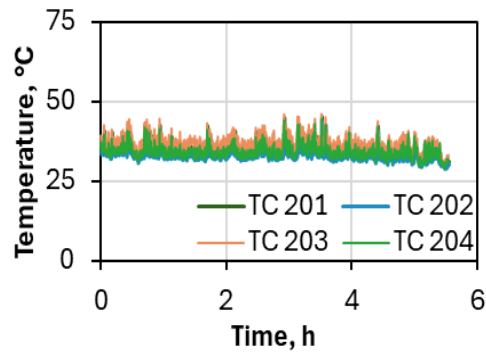
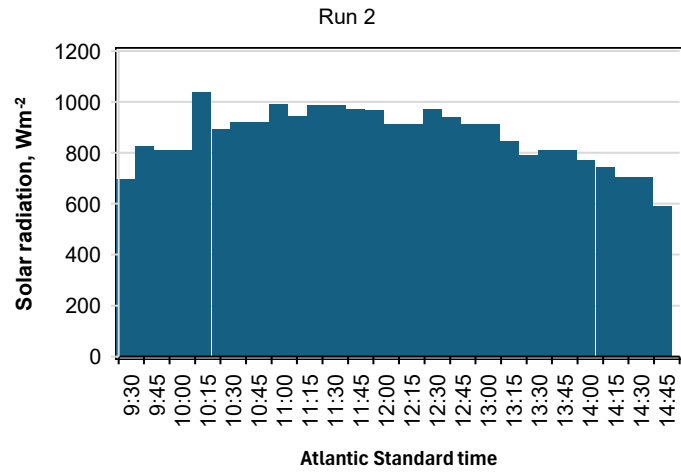


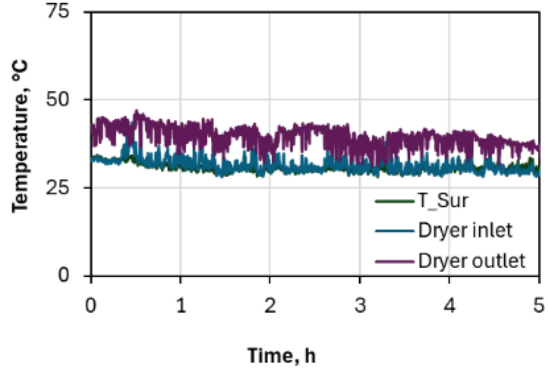
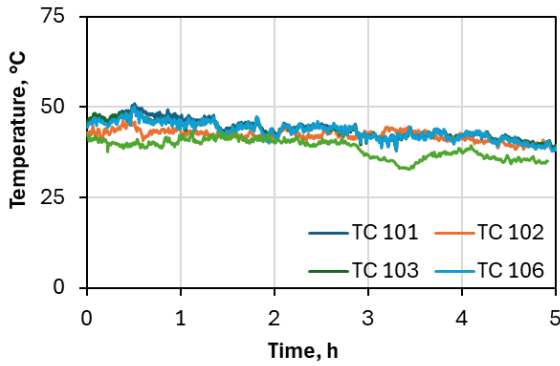
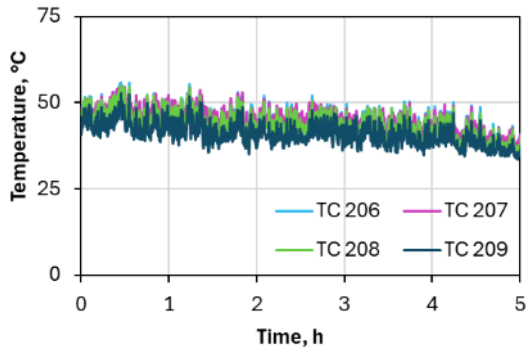
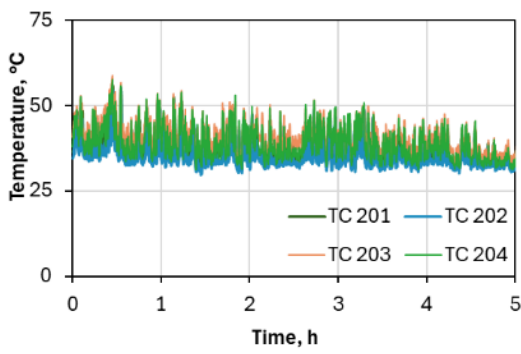
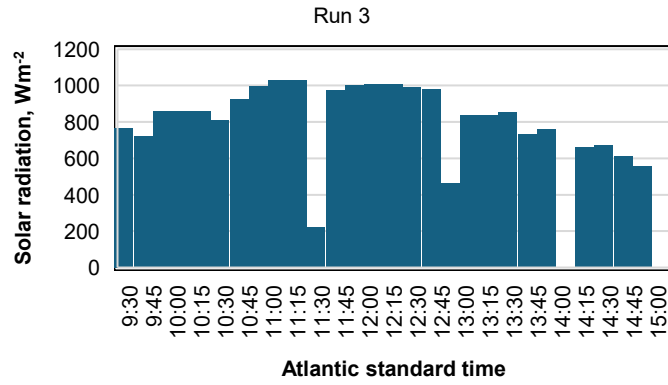
Outlet speed distribution while drying 5 mm thick sample (Run 1)



Outlet speed distribution while drying 5 mm thick sample (Run 2)

Appendix C: Solar radiation measurements and temperature distribution in a dryer





References

- Belessiotis, V., & Delyannis, E. (2011). Solar drying. *Solar Energy, Progress in Solar Energy* 1, 85(8), 1665–1691. <https://doi.org/10.1016/j.solener.2009.10.001>
- Buzrul, S. (2022). Reassessment of Thin-Layer Drying Models for Foods: A Critical Short Communication. *Processes*, 10(1). <https://doi.org/10.3390/pr10010118>
- Caballero-Cerón, C., Guerrero-Beltrán, J. A., Mújica-Paz, H., Torres, J. A., & Welti-Chanes, J. (2015). *Moisture Sorption Isotherms of Foods: Experimental Methodology, Mathematical Analysis, and Practical Applications* (pp. 187–214). https://doi.org/10.1007/978-1-4939-2578-0_15
- DM Aruba. (2020). *Aruba climatological summary 2020*. Departamento Meteorológico Aruba. https://www.meteo.aw/files/Download/aruba_rep_2020.pdf
- El-Beltagy, A., Gamea, G. R., & Essa, A. H. A. (2007). Solar drying characteristics of strawberry. *Journal of Food Engineering*, 78(2), 456–464. <https://doi.org/10.1016/j.jfoodeng.2005.10.015>
- Elwakeel, A. E., Oraith, A. A. T., Gameh, M. A., Eissa, A. S., Mahmoud, S. F., Eid, M. H., Moussa, A., Mostafa, M. B., Taha, M. F., Abulmeaty, S. A. T., & Tantawy, A. A. (2025). Quality evaluation of dried tomato fruit and optimization of drying conditions using a modified solar dryer integrated with an automatic solar collector tracker. *Scientific Reports*, 15(1), 7659. <https://doi.org/10.1038/s41598-025-89248-x>
- Ennissioui, J., Benghoulam, E. M., & El Rhafiki, T. (2023). Experimental study of a natural convection indirect solar dryer. *Heliyon*, 9(11), e21299. <https://doi.org/10.1016/j.heliyon.2023.e21299>
- Getie, M. Z., Tadesse, M., & Alemu, M. A. (2025). Design, manufacturing, and performance evaluation of box-type direct solar dryer for onions (*Allium cepa* L.). *Cogent Engineering*, 12(1), 2574531. <https://doi.org/10.1080/23311916.2025.2574531>

- Henderson, S. M., & Pabis, S. (1961). Grain drying theory 1. Temperature effect on drying coefficient. *Journal of Agricultural Engineering Research*, 6(3), 169-74 ref. bibl. 14.
- Kort, R. de, Obispo, S., Carmona Báez, A., Echteld, E., & Mijts, E. (2024). *Strengthening Economic Resilience in Small Island States: A Situational Analysis of Food Entrepreneurship, with a Focus on the Cucumis Anguria Cucumber in Aruba*. University of Curaçao/University of Puerto Rico.
- Kumar, M., Sansaniwal, S. K., & Khatak, P. (2016). Progress in solar dryers for drying various commodities. *Renewable and Sustainable Energy Reviews*, 55, 346–360.
<https://doi.org/10.1016/j.rser.2015.10.158>
- Meghwar, B. L., Khan, A., Lakhiar, I. A., Mirani, A. A., Daper, M. S., & Kalroo, M. W. (2023). Comparison Between Solar Tunnel, Solar-Cum Gas Dryer, and Open Sun Drying Methods for Drying Red Chillies. *Pakistan Journal of Agricultural Research*, 36(1).
<https://doi.org/10.17582/journal.pjar/2022/36.1.63.70>
- Mimmi, S. F., Saha, C. K., Akter, T., Kabir, M., & Khatun, Mst. L. (2025). Solar Dryer for Drying Cabbage in Single and Multilayers. *Journal of Food Processing and Preservation*, 2025(1), 6677702. <https://doi.org/10.1155/jfpp/6677702>
- Mohapatra, S. S., & Mahanta, P. (2012). Performance Evaluation of Quality Drying in a Natural Convection Grain Dryer. *Applied Mechanics and Materials*, 110–116, 2094–2100.
<https://doi.org/10.4028/www.scientific.net/AMM.110-116.2094>
- Mugi, V. R., & V. P., C. (2022). Comparison of drying kinetics, thermal and performance parameters during drying guava slices in natural and forced convection indirect solar dryers. *Solar Energy*, 234, 319–329. <https://doi.org/10.1016/j.solener.2022.02.012>
- Olabi, A. G., Elsaid, K., Obaideen, K., Abdelkareem, M. A., Rezk, H., Wilberforce, T., Maghrabie, H. M., & Sayed, E. T. (2023). Renewable energy systems: Comparisons, challenges and barriers, sustainability indicators, and the contribution to UN sustainable

- development goals. *International Journal of Thermofluids*, 20, 100498.
<https://doi.org/10.1016/j.ijft.2023.100498>
- Omolola, A. O., Jideani, A. I. O., & Kapila, P. F. (2014). Modeling microwave drying kinetics and moisture diffusivity of Mabonde banana variety. *International Journal of Agricultural and Biological Engineering*, 7(6), 107–113. <https://doi.org/10.25165/ijabe.v7i6.1267>
- Park, J., Yeom, J., Baeck, S., Lee, S., & Park, J. Y. (2025). A Numerical Analysis of Flow Dynamics Improvement in a Blower via Simple Integration of Bell Mouth and Nose Cone Structures. *Energies*, 18(7), 1830. <https://doi.org/10.3390/en18071830>
- Rehman, S., & Rubab, S. (2022). Solar radiation impact on drying parameters of mint (*Mentha spicata* L.). *International Journal of Health Sciences*, 6(S6), 3235–3246.
<https://doi.org/10.53730/ijhs.v6nS6.10053>
- Ren, Q., Fang, J., & Zhao, Y. (2025). Prediction Method of Tangerine Peel Drying Moisture Ratio Based on KAN-BiLSTM and Multimodal Feature Fusion. *Applied Sciences*, 15(11), 6130. <https://doi.org/10.3390/app15116130>
- Riadh, M. H., Ahmad, S. A. B., Marhaban, M. H., & Soh, A. C. (2015). Infrared Heating in Food Drying: An Overview. *Drying Technology*, 33(3), 322–335.
<https://doi.org/10.1080/07373937.2014.951124>
- Schudel, S., Shoji, K., Shrivastava, C., Onwude, D., & Defraeye, T. (2023). Solution roadmap to reduce food loss along your postharvest supply chain from farm to retail. *Food Packaging and Shelf Life*, 36, 101057. <https://doi.org/10.1016/j.fpsl.2023.101057>
- Shalaby, S. M., & Bek, M. A. (2014). Experimental investigation of a novel indirect solar dryer implementing PCM as energy storage medium. *Energy Conversion and Management*, 83, 1–8. <https://doi.org/10.1016/j.enconman.2014.03.043>
- Singh, A. P., Akshayveer, Kumar, A., & Singh, O. P. (2019). Designs for high flow natural convection solar air heaters. *Solar Energy*, 193, 724–737.
<https://doi.org/10.1016/j.solener.2019.10.010>

- Tawfik, M. A., Oweda, K. M., Abd El-Wahab, M. K., & Abd Allah, W. E. (2023). A New Mode of a Natural Convection Solar Greenhouse Dryer for Domestic Usage: Performance Assessment for Grape Drying. *Agriculture*, 13(5), 1046.
<https://doi.org/10.3390/agriculture13051046>
- Tepe, T. K. (2024). Convective Drying of Potato Slices: Impact of Ethanol Pretreatment and Time on Drying Behavior, Comparison of Thin-Layer and Artificial Neural Network Modeling, Color Properties, Shrinkage Ratio, and Chemical and ATR-FTIR Analysis of Quality Parameters. *Potato Research*, 67(3), 759–783. <https://doi.org/10.1007/s11540-023-09663-3>
- UNDP. (2024). *Small Island Developing States are on the frontlines of climate change – here’s why* | UNDP Climate Promise. <https://climatepromise.undp.org/news-and-stories/small-island-developing-states-are-frontlines-climate-change-heres-why>
- UNDP. (2025). *Renewable energy – powering a safer future*. United Nations. United Nations. <https://www.un.org/en/climatechange/raising-ambition/renewable-energy>
- Vijaya Venkata Raman, S., Iniyar, S., & Goic, R. (2012). A review of solar drying technologies. *Renewable and Sustainable Energy Reviews*, 16(5), 2652–2670.
<https://doi.org/10.1016/j.rser.2012.01.007>
- Werner Mühlbauer & Joachim Müller. (2020). Drying kinetics. In *Drying Atlas—Drying Kinetics and Quality of Agricultural Products* (pp. 53–61). <https://doi.org/10.1016/B978-0-12-818162-1.00002-X>
- Zang, Y., & Mittal, G. (2005). Inactivation of spoilage microorganisms in mango juice using low energy pulsed electric field in combination with antimicrobials. *Italian Journal of Food Science*, 17(2), 167–176.